

## Modified Cap Model with Linear Kinematic Hardening for Dynamic Behaviour of Sand

S. Teachavorasinskun<sup>1</sup>, F. Tanizawa<sup>1</sup> and T. Sueoka<sup>1</sup>

### ABSTRACT

The constitutive soil model called 'Combined Surface model (CS)' is implemented into the newly developed analysis system (SYSTEM-L) which can carry out pre-processing, FEM analysis and post processing. The CS model is formulated using three different yield surfaces which will be activated at a proper time. The first surface is modified from the conventional associated cap surface. Utilization of this enables the model to predict the effect of consolidation and initial pressure levels. When stress reversal takes place or when the stress point is located inside the bounding cap surface, a circular surface incorporated with the kinematic hardening rule is activated to evaluate the plastic deformation. The kinematic hardening rule is expressed as a function of the stresses at the reversal point and the plastic strains. Finally the non-associated Drucker-Prager yield surface is employed if the stress ratio exceeds the phase transformation line. The excessive dilatancy incorporate with the conventional D-P model is reduced by using of the proposed plastic potential function which approaches the von-mises criteria when mean stress becomes large. In this paper, the description for the model will be given, then, the calculated results are compared to those obtained from the triaxial tests.

### INTRODUCTION

Resistance of sand deposits to liquefaction is one of the most important factors determining the stability of the structures it supports. Several factors influencing the liquefaction characteristic of soils have been extensively investigated using both laboratory apparatuses and field measurements. These include the relative density of the deposit, grain characteristics, soil structure, previous strain history and etc (Seed, 1976). Based on these extensive investigations, simple physical models or complex constitutive soil models have been established. It should be noted that investigation of liquefaction of soil in the laboratory is mostly dependent on the using of the simple shear test and triaxial test apparatuses. Since these two apparatuses create different stress paths, the formulations based solely on the results of one of these two tests would provide an erroneous when dealing with natural sand deposits. A good constitutive equation should be able to, at least, predict the results provided by both tests, though, the prediction under mixing condition is preferred in evaluating effects of two-dimensional stress field. Furthermore, effects of pore water pressure need to be considered; i.e., effective stress analysis is preferred. This can be achieved in two fashions; that is a coupled technique using Biot's two phase formulation or an un-coupled technique where the excess pore water pressure is calculated using a separated pore water pressure model.

It has been widely accepted that non-linear behavior of soil plays an important role in the predictability of the analysis. The non-linear elastic model such as the hyperbolic and the Ramberg-Osgood equations with the second-masing rule for expressing its cyclic behavior is a simpler way comparing to the elasto-plastic model. Some modifications are required when elasto-plastic concept is employed, since the conventional elasto-plastic assumes no plastic deformation during unloading.

1) Research Engineer, Technology Research Center, Taisei Corporation, Yokohama, Japan.

The direct non-linear method, which includes a pore water pressure generation model to permit effective stress analysis, tracks the hysteretic non-linear stress-strain paths continuously during cyclic loading and unloading. Seed et al.(1975) linked the dynamic analysis of the soil skeleton and the pore water pressure response calculations by the equivalent uniform shear stress cycles. If the equivalent shear stress cycle,  $N_{eq}$ , is defined as the number of uniform stress cycles undergone by the soil during the earthquake period and  $N_1$  is the number of cycle at the same stress level required to cause liquefaction under undrained uniform cyclic loading condition. The pore water pressure build-up can be determined as a function of the ratio between  $N_{eq}$  and  $N_1$ . Analyses of pore water pressure response to earthquake using such model was carried out by Chugh and Thun (1985).

Martin et al.(1975) proposed that the intergranular contact forces induced during the shear strain cycle in undrained condition are similar to those induced during drained cycle. However, the slip deformation must transfer some of the vertical stress previously carried by the intergranular forces to the more incompressible water. Therefore, the change in volume of voids must equal to the net change in volume of sand structure. Both of them can be proportionally related through the bulk modulus of water, the tangent modulus determined from one-dimensional unloading test and the porosity of the sample. Implementation this pore water generation model with the hyperbolic stress-strain relationship, the equations of motion of the discrete mass system was solved (Finn et al.1977). Several other non-linear stress-strain and pore water pressure models were proposed; e.g., Fukutake et al.1990, Matasovic et al.1992.

Plasticity models based on the classical isotropic hardening concept such as the Cam Clay models (Roscoe, Schofield and Wroth (1958) and Burland (1965) cannot simulate the pore water pressures generated during cyclic loading. Conventionally, the yield surface was allowed to contract during unloading due to the overconsolidation to simulate this effect. Mroz and Norris (1982) proposed the multi-surface hardening model which allows translation each yield surface. Dafalias and Hermann (1982) used the bounding surface concept to predict the pore water pressure when stress point is located inside the bounding surface. Another techniques can be found in the literatures; such as, Oka et al.1981, Ghaboussi and Momen, 1984 and Prevost, 1978.

In the present paper, the details Combined Surface Model (CS model) will be presented. The performance of the model is, then, calibrated using static and cyclic test results obtained from the laboratory.

#### COMBINED SURFACE MODEL

Baladi and Rohani (1979) proposed that the yield surface of soil takes an elliptic shape as shown in Fig.1 in which  $I_1$  and  $J_2$  are the first and second invariant stress tensors, respectively. Note that the surface makes an right angle to the mean stress axis and the failure line. In the present study, the curvature of the ellipse is assumed to be a function of location of the cap. The modified form of the proposed yield surface is shown in Eq.(1).

$$f_c = (I_1 - L)^2 + \left( R \left( \frac{X}{X_{ini}} \right)^m \right)^2 J_2 - (X - L)^2 = 0 \quad (1)$$

where  $X$  is the hardening parameter depending on the stress states and plastic volumetric strain,  $R$  is the initial curvature of the ellipse and  $L$  and  $m$  are material constants. The physical expression for some parameters are shown in Fig.1(a). The second term of the middle expression was implemented in order that the effects of initial confining pressure could be taken into account, since sand having higher confining stress is more likely to flow than that having lower confining pressure (Ishihara, 1993). In the other word, the effective stress paths for soil having different initial stresses are not symmetric as schematically shown in Fig.1(b).

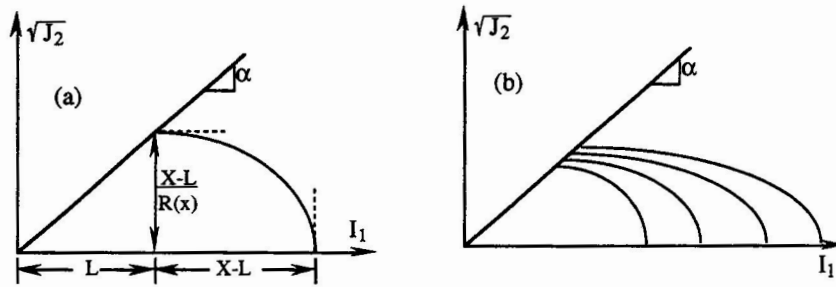


Fig.1 (a) The physical meanings of some parameters of the modified cap model; (b) Schematic diagram showing the effects of the initial confining stress on the stress path of sand.

The associated flow rule was used to calculate the plastic strain increment for this surface; i.e., the plastic potential surface is the same as the yield surface. Expression for the hardening parameter,  $X$ , which in turn identified the location of the current cap surface, is determined using the results obtained from the laboratory tests. It was found that the relationship between the  $M_v^t/(1+e_0)$  and the  $p'/p_0$  for sample with different initial conditions are unique as shown in Fig.2, where  $M_v^t$  is the ratio between the increment of total volumetric strain,  $d\varepsilon_v^t$ , to the increment of effective mean stress,  $dp'$ , and  $e_0$  and  $p_0$  are the initial void ratio and initial mean effective stress, respectively.  $M_v^t$  could be expressed as the inverse value of the bulk modulus. Note that the formulation proposed by Hardin (1972) and Tanizawa et al. (1994) were employed in calculation of elastic component.

$$d\varepsilon_i^e = \frac{1}{K_e} \left( \frac{d\sigma_i}{\sigma_i^n} - \nu \frac{d\sigma_j}{\sigma_j^n} - \nu \frac{d\sigma_k}{\sigma_k^n} \right)$$

where  $d\varepsilon_i^e$  is the elastic strain increment in the direction of  $d\sigma_i$  and  $\nu$  is the poisson's ratio.  $K_e$  is the initial Young's modulus,  $E_{max}$ , determined at  $p'=1.0$  kgf/cm<sup>2</sup>. For the case of isotropic consolidation,  $d\sigma_1 = d\sigma_2 = d\sigma_3 = dp'$  and  $\sigma_1 = \sigma_2 = \sigma_3 = p'$ , the above equation can be simply expressed as;

$$\frac{d\varepsilon_v^e}{dp'} = \frac{3(1-2\nu)}{K_e p'^n} \quad (2)$$

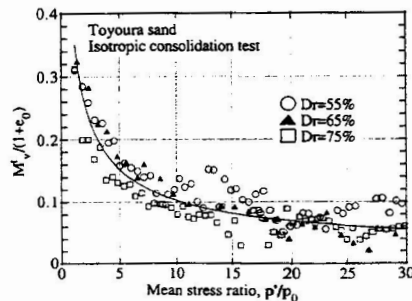


Fig.2 A unique relationship between the function of plastic strain and mean effective stress.

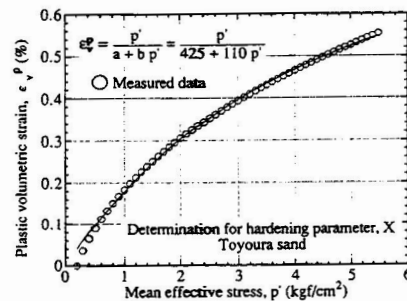


Fig.3 Example of using of hyperbolic fitting for hardening parameter.

The plastic strain component, then, is calculated using the elastic equation (Eq.(2)) and the total strain formulation as shown in Fig.2. For simplicity, hardening parameter  $X$  is again related to the total plastic strain,  $\varepsilon_v^p$ , using the hyperbolic equation which was controlled by two parameters,  $a$  and  $b$ . It should be

noted that parameters  $a$  and  $b$  are not additional parameters but they were automatically derived from the above procedure. The example of the fitting for Toyoura sand sample having initial void ratio of 0.75 is shown in Fig.3. For the details of the derivation of this yield surface see Sueoka et al.(1994).

The second surface used in the model is the circular surface with constant radius; i.e., no isotropic expansion of the surface. The kinematic hardening parameter which is a function of the plastic strains,  $\epsilon_{ij}^p$ , and the stress at reversal point,  $(\sigma_{ij})^*$  is used to calculate the increment of plastic deformation associated with this surface. This surface could be expressed as;

$$f_r = (I_1 - \alpha_{kk})^2 + (J_2 - \beta) = k$$

or

$$f_r = (\bar{I}_1)^2 + \bar{J}_2 = k$$

where  $\alpha_{kk}$  and  $\beta$  are the kinematic hardening parameters which could be expressed using the linear kinematic rule as;

$$\alpha_{ij} = (\sigma_{ij})^* - D \epsilon_{ij}^p \quad \text{and} \quad d\alpha_{ij} = -D d\epsilon_{ij}^p$$

since

$$\bar{I}_1 = \bar{\sigma}_{ij} \delta_{ij} = (\sigma_{ij} - \alpha_{ij}) \delta_{ij}$$

where  $(\sigma_{ij})^*$  is the stress tensor when stress reversal takes place. From the above equation,  $\alpha_{kk}$  could be determined as;

$$\alpha_{kk} = \alpha_{ij} \delta_{ij} = I_1^* - D \epsilon_{ij}^p \delta_{ij} = I_1^* - D \epsilon_v^p$$

Similar expression could be derived for the deviatoric stress component,  $s_{ij}$ , as;

$$\bar{s}_{ij} = s_{ij} - \left( \alpha_{ij} - \frac{1}{3} \alpha_{kk} \delta_{ij} \right)$$

The explicit form of  $\beta$  is more complicated, however, it is not necessary in performing the analysis. In this paper, only the formulation of  $\beta$  under triaxial condition will be given;

$$\beta = \frac{1}{3} (\alpha_{11} - \alpha_{22}) (2(\sigma_{11} - \sigma_{22}) - (\alpha_{11} - \alpha_{22}))$$

The kinematic hardening modulus,  $H'_k$ , could be determined using the consistency condition of the yield surface as;

$$df_r = \frac{\partial f_r}{\partial \sigma'_{ij}} d\sigma'_{ij} - \frac{\partial f_r}{\partial \sigma'_{ij}} \frac{\partial \alpha_{ij}}{\partial \epsilon_{ij}^p} d\epsilon_{ij}^p = 0 \quad (3)$$

And the plastic strain determined from the associated flow rule as;

$$d\epsilon_{ij}^p = d\lambda \frac{\partial f_r}{\partial \sigma'_{ij}} = \frac{1}{H'_k} \left( \frac{\partial f_r}{\partial \sigma'_{mn}} d\sigma'_{mn} \right) \frac{\partial f_r}{\partial \sigma'_{ij}}$$

Substituting this into Eq.(3), the kinematic hardening modulus is derived.

$$H'_k = -D \frac{\partial f_r}{\partial \sigma_{kl}} \frac{\partial f_r}{\partial \sigma_{mn}}$$

It can be seen that  $H'_k$  is dependent on the parameter D. It should be noted that as plastic strain developed during stress reversal, the cap (bounding) surface is also expanding accordingly to the current plastic volumetric strain. If the stress point is going to move beyond the current cap surface, the reversal surface is frozen while the cap surface is re-activated.

The last surface implemented into the CS model is the Drucker-Prager surface. Since the using of associated flow rule could result in excessive dilatancy, the non-associated flow rule is adopted. The yield and the proposed plastic potential functions can be expressed as;

$$f_f = \sqrt{J_2} - \alpha I_1 = 0$$

$$g_f = \sqrt{J_2} - A(1 - e^{-B I_1})$$

The potential surface approaches the von-mises criteria when the mean stress becomes large ( $J_2 = A^2$ ). The schematic diagram showing these two surface on the two-dimensional stress space is shown in Fig.4.

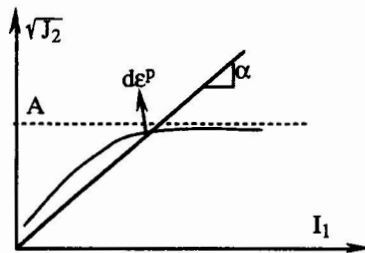


Fig.4 Schematic diagram showing the proposed plastic potential surface for D-P yield surface.

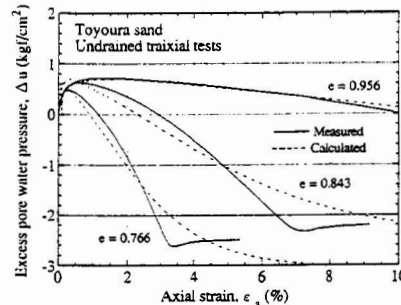


Fig.5 Comparison of the measured and predicted pore water pressure during static loading tests.

#### COMPARISON WITH TEST DATA

A series of monotonic and cyclic triaxial tests were carried out in order to calibrate the proposed CS model. Fig.5 shows the comparison between the measured and predicted excess pore water pressure developed during static monotonic compression test of Toyoura sand. It can be seen that the model could predict well both the contractive and dilative behavior of sand. The details of the parameters for the static monotonic test was reported in Sueoka et al.(1994).

For the simulation of the undrained cyclic loading test, the parameter D needed to be determined. The fitting procedure for determination of this parameter is required. Conventional method using the liquefaction strength at 20 cycles of cyclic loading was employed for the fitting. After parameter D is determined, the liquefaction potential for other cyclic stress ratios were calculated to form the liquefaction potential curve. Two densities,  $D_r = 55$  and  $75\%$ , of Toyoura sand were tested and used for calibration. The values of D for loose and dense samples are 1000 and 1400, respectively. The effective stress paths and the shear stress and shear strain predicted by the model for dense samples are shown in Fig.6 and 7. Note that when the cyclic stress ratio,  $q/2\sigma_v$ , is equal to 0.1, there is no liquefaction or cyclic mobility

taken place for both densities. The maximum pore pressure ratio is about 0.45 for dense sample. When the cyclic stress ratio becomes 0.2, cyclic mobility was predicted. One shortcoming of the model is that the developed shear strain is a little bit too small compared to those measured in the laboratory.

Fig.8 shows the comparison between the liquefaction potential curves measured in the laboratory to those calculated by the proposed model. It can be seen that the model could predict well the liquefaction strength curve both at large and small cyclic stress ratios.

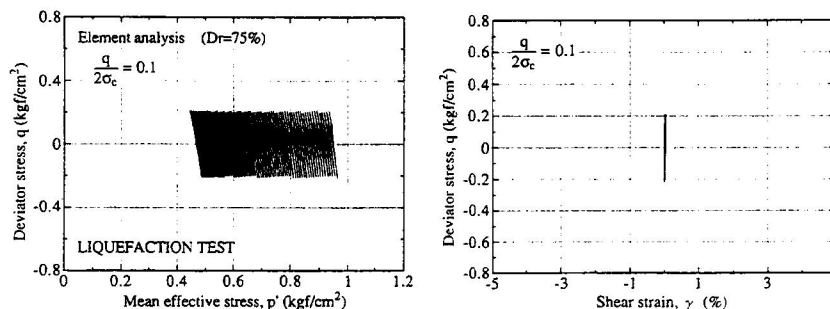


Fig.6 Effective stress path and cyclic stress-strain relationship obtained at cyclic stress ratio of 0.1

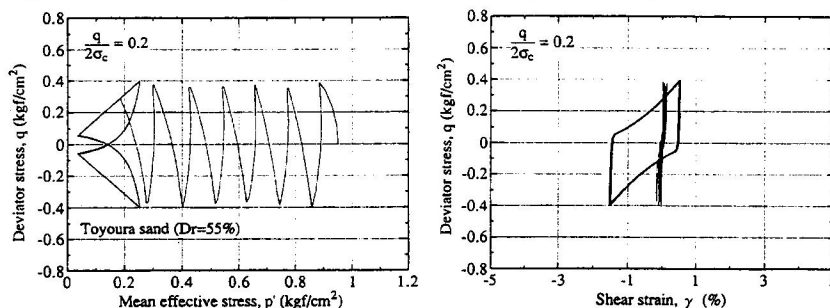


Fig.7 Effective stress path and cyclic stress-strain relationship obtained at cyclic stress ratio of 0.2

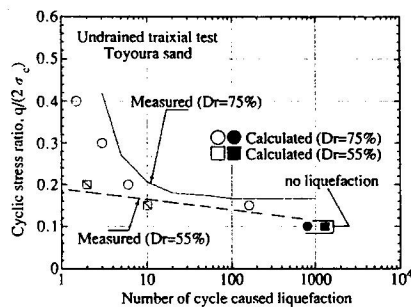


Fig.8 Measured and predicted liquefaction strength curves

### CONCLUSIONS

By implementing the plastic potential surface, the proposed CS model could simulate well both the contractive and dilative behaviors of sand. Also the concepts of kinematic hardening and the bounding surface enabled the model to simulate plastic deformation during stress point located inside the yield

surface. It was found that the liquefaction curves can be well predicted by the model, especially when small cyclic stress ratio was used.

#### REFERENCES

- Baladi, G. Y. and Rohani, B. 1979. Elasto-plastic model for saturated sand. *Journal of the Geotechnical Engineering Division, ASCE*, Vol.105, pp.465-480.
- Burland, J. B. 1965. The yielding and dilation of clay. *Correspondence, Geotechnique*, Vol.15, pp.211-214.
- Chugh, A. K. and Thun, J. L. V. 1985. Pore pressure response analysis for earthquakes. *Canadian Geotechnique*, Vol.22, pp.466-476.
- Dafalias, Y. F. and Hermann, L. R. 1982. Bounding surface formulation of soil plasticity. *Soil Mechanics-Transient and cyclic loads*, Edited by G.N.Pande and O.C.Zienkiewicz, John Wiley & Sons, Ltd., pp.253-282.
- Finn, W. D. L., Lee, K. W. and Martin, G. R. 1976. An effective stress model for liquefaction. *Journal of the Geotechnical Engineering Division, ASCE*, Vol. 103, No.GT6, June, pp.517-533.
- Fukutake, K., Akira, O., Masayoshi, S. and Shamoto, Y. 1990. Analysis of saturated dense sand-structure system and comparison with results from shaking table test. *Earthquake Engineering and Structural Dynamics*, Vol.19, pp.977-992.
- Ghaboussi, J. and Momen, H. (1982): " Modeling and analysis of cyclic behavior of sands," *Soil Mechanics-Transient Loads*, Edited by G.N.Pande and O.C.Zienkiewicz, John Wiley & Sons Ltd., pp.313-342.
- Hardin, B. O. 1978. The nature of stress-strain behavior of soils. *Earthquake Engineering and Soil Dynamics, ASCE, Pasadena*, June, pp.3-89.
- Ishihara, K. 1992. Liquefaction and flow failure during earthquake. Rankine Lecture, *Geotechnique*, Vol.43, No.3, pp.349-415.
- Martin, G. R., Finn, W. D. L. and Seed, H. B. 1975. Fundamentals of liquefaction under cyclic loading. *Journal of the Geotechnical Engineering Division, ASCE*, Vol.101, No.GT6, May, pp.423-438.
- Matasovic, N. and Vucetic, M. 1992. Cyclic characterization of liquefiable sands. *Journal of the Geotechnical Engineering Division, ASCE*, Vol.119, No.11, November, pp.1805-1822.
- Mroz, Z. and Norris, V. A. 1982. Elastoplastic and viscoplastic constitutive models for soils with application to cyclic loading. *Soil Mechanics-Transient and cyclic loads*, Edited by G.N.Pande and O.C.Zienkiewicz, John Wiley & Sons, Ltd., pp.173-217.
- Oka, F., Sekiguchi, K. and Goto, H. 1981. A method of analysis of earthquake-induced liquefaction of horizontally layered sand deposits. *Soils and Foundations*, Vol.21, No.3, pp.1-17.
- Schofield, A.N. and Wroth, C.P. (1972): " Critical state soil mechanic," McGraw-Hill.
- Seed, H. B. 1976. Evaluation of Soil Liquefaction Effects on Level Ground During Earthquake. *Liquefaction Problems in Geotechnical Engineering, ASCE National Convention, September, Philadelphia*, pp. 1-104.
- Seed, H. B., Idriss, I. M., Makdisi, F. and Banerjee, N. 1975. Representation of irregular stress time histories by equivalent uniform stress series in liquefaction analyses. *Earthquake Engineering Research Center, University of California, Berkeley, CA, Report No. EERC 75-29*.
- Tanizawa, F., Sueoka, S., Yamaguchi, J., Sueoka, T. and Goto, S. 1994. Measurement of shear wave velocity before liquefaction and during cyclic mobility. *International Symposium on Pre-Failure Deformation of Geomaterials, September, IS' HOKKAIDO, Japan*.
- Sueoka, T., Teachavorasinskun, S. and Tanizawa, F. 1994. Small to large strain level behaviors of sand by elasto-plastic model. *International Symposium on Pre-Failure Deformation of Geomaterials, September, IS' HOKKAIDO, Japan*.